Analytica Chimica Acta 1385 (2026) 345001

Contents lists available at ScienceDirect

Analytica Chimica Acta

journal homepage: www.elsevier.com/locate/aca

Ionic-liquid-based aqueous biphasic systems meet microfluidics: from antibodies to aptamers in prostate-specific antigen detection

Maria S.M. Mendes [a,b], Virginia Chu [b], Mara G. Freire [a], Francisca A. e Silva [a,*], João P. Conde [b,c,**]

[a] CICECO – Aveiro Institute of Materials, Department of Chemistry, University of Aveiro, Aveiro, Portugal
[b] Instituto de Engenharia de Sistemas e Computadores – Microssistemas e Nanotecnologias (INESC MN), Lisbon, Portugal
[c] Department of Bioengineering, Instituto Superior Técnico, Universidade de Lisboa, Lisbon, Portugal

HIGHLIGHTS

- Ionic liquid aqueous biphasic systems are combined with microfluidics to detect PSA.
- Antibodies and aptamers are compared as recognition elements in microfluidic assays.
- Depletion of high-abundance proteins reduces matrix effects and restores sensitivity.
- Aptamers enable PSA detection at clinically relevant levels, surpassing antibodies.

GRAPHICAL ABSTRACT

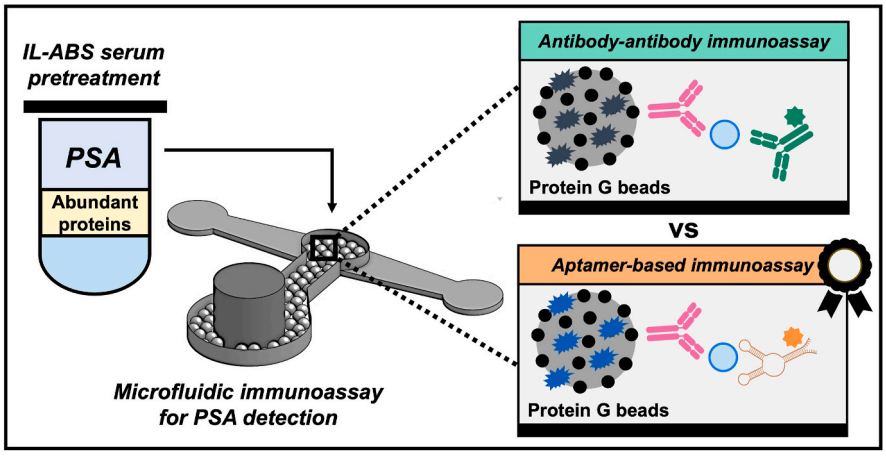

ARTICLE INFO

Keywords:
Prostate-specific antigen
Sample pretreatment
Aqueous biphasic system
Microfluidic device
Aptamer

ABSTRACT

Background: Prostate-specific antigen (PSA) is the most widely used biomarker for prostate cancer screening; still, its reliable quantification in human serum remains challenging due to matrix complexity and high-abundance proteins that interfere with target recognition and signal generation. These limitations reduce the performance of biosensing microfluidic platforms. Ionic-liquid-based aqueous biphasic systems (IL-ABS) have been proposed as effective serum pretreatment tools, enabling selective depletion of high-abundance proteins, analyte preconcentration, and seamless integration with microfluidic devices. However, the synergistic combination of IL-ABS with microfluidic immunoassays has so far been restricted to antibody-based formats, which are limited in stability, cost, and target accessibility.

Results: Here, the analytical scope of the combined IL-ABS pretreatment and microfluidic detection platform is expanded beyond conventional antibody-based formats by introducing aptamers as recognition elements. The

* Corresponding author.
** Corresponding author. Instituto de Engenharia de Sistemas e Computadores – Microssistemas e Nanotecnologias (INESC MN), Lisbon, Portugal.
E-mail addresses: francisca.silva@ua.pt (F.A. e Silva), joao.conde@tecnico.ulisboa.pt (J.P. Conde).

https://doi.org/10.1016/j.aca.2025.345001
Received 29 October 2025; Received in revised form 26 November 2025; Accepted 8 December 2025
Available online 10 December 2025

resulting aptamer-based sandwich immunoassay was benchmarked against the conventional antibody-antibody format, demonstrating superior sensitivity and a limit of detection of 7.49 ng mL^{-1}, within the clinically relevant range for PSA screening.

Significance: This work pioneers the combined use of IL-ABS pretreatment and aptamer-based microfluidic detection for PSA. Aptamers, as synthetic ligands, offer high specificity, enhanced stability, and flexible design, providing a cost-effective alternative to antibodies. Incorporating aptamer recognition enhances analytical performance relative to conventional antibody-based assays, highlighting the platform's potential for broader clinical and point-of-care applications.

1. Introduction

Prostate cancer is among the most frequently diagnosed oncologic diseases, remaining a leading cause of cancer-related mortality worldwide [1]. Its early detection relies primarily on prostate-specific antigen (PSA), the established clinical biomarker for diagnosis, prognosis, and therapeutic follow-up [2]. While PSA concentrations below 4 ng mL^{-1} are typical in healthy individuals, cancer patients often show substantially elevated levels, demanding analytical solutions with exceptional sensitivity and precision [3]. Conventional immunoassays remain the standard practice for PSA quantification due to their robustness and long-recognized clinical reliability [4]. However, these protocols are inherently resource-intensive, which limits their applicability in rapid diagnostics and decentralized healthcare [4]. In response, microfluidic lab-on-a-chip platforms have emerged as promising alternatives for PSA detection, combining miniaturization, reduced reagent consumption, accelerated analysis, and compatibility with point-of-care testing [5,6].

Recent microfluidic strategies for PSA detection have increasingly focused on improving analytical sensitivity, reducing assay time, and enabling point-of-care deployment. These rely on the integration of sandwich-type immunoassays with diverse transduction mechanisms, including electrochemical, optical, and fluorescence readouts [7]. Early antibody-based microfluidic platforms demonstrated enhanced sensitivity and reduced assay times compared with conventional enzyme-linked immunosorbent assays (ELISA), with some electrochemical designs achieving detection within seconds [8–10]. Progress in the field led to the introduction of aptamers, i.e., short, single-stranded DNA or RNA sequences that fold into defined three-dimensional structures capable of binding to target molecules with high specificity and affinity [11]. Unlike antibodies, which are traditionally produced in animals or derived from animal cell lines and require labor-intensive production with potential batch-to-batch variability, aptamers are generated via the SELEX process (Systematic Evolution of Ligands by Exponential Enrichment), enabling fine-tuned control over their binding properties [11,12]. Aptamers exhibit superior chemical stability, are readily modified with functional groups and can be synthesized in a straightforward, cost-effective, and highly reproducible manner [11,12]. These features allow aptamer-based microfluidic biosensors to reach detection limits in the picogram-per-milliliter and even femtomolar range, while maintaining reliable performance in complex samples [13,14].

Despite substantial progress in microfluidic PSA detection, analytical performance remains constrained by the intrinsic complexity of human serum, especially due to high-abundance proteins such as human serum albumin (HSA) and immunoglobulin G (IgG) that induce non-specific binding and signal attenuation. Sample pretreatment is therefore essential to remove these interfering proteins and restore assay specificity and sensitivity [15,16]. However, identifying strategies that are both compatible with microfluidic devices and suitable for point-of-care implementation remains challenging. While solid-phase extraction (SPE) is widely used due to its efficiency and adaptability to miniaturization, it often depends on costly affinity ligands and involves complex elution steps that hinder direct sample processing [17]. Aqueous biphasic systems (ABS), a fully aqueous liquid-liquid extraction approach, have emerged as a promising option, particularly due to their biocompatibility and gentle partition environment [18]. While traditional ABS rely on polymers and salts as phase-forming components [19,20], the use of hydrophilic ionic liquids (ILs) introduces greater structural diversity, offering sharper tunability in phase behavior and enhanced selectivity in biomolecule separation [21,22]. In particular, ABS based on ILs (hereafter referred to as IL-ABS) enable simultaneous depletion of high-abundance proteins and quantitative PSA recovery from serum in a single step, with biomarker losses within regulatory limits [23]. Additionally, IL-ABS show strong synergy with microfluidic platforms, allowing streamlined sample processing and enhancing immunoassay sensitivity. As a result, lower PSA detection limits are achievable compared with analyses performed on untreated serum [24].

Although IL-ABS have proven effective in microfluidic platforms, this synergy has thus far been largely confined to antibody-based detection [24]. To expand its potential, the present work introduces the combination of IL-ABS serum pretreatment with a microfluidic aptamer-based detection strategy. Aptamer-based and antibody-based formats are directly compared to assess sensitivity and performance in both phosphate-buffered saline (PBS) and complex serum matrices. In addition, while previous approaches achieved PSA detection at clinically relevant concentrations, the detection chamber's relatively large, yet functional, design indicated room for dimensional optimization [24]. Accordingly, a redesigned microfluidic chamber is introduced in this work.

2. Materials and methods

2.1. Materials

For the development of the microfluidic immunoassay, Protein G Sepharose® 4 Fast Flow microbeads were purchased from Cytiva. As blocking agents, purified human IgG solution (29.4 mg mL^{-1}) was sourced from Innovative Research, Inc., and Tween® 20 was purchased from Sigma-Aldrich. PSA from human semen (P3235), the anti-PSA mouse monoclonal capture antibody (MABX5532), and the anti-PSA mouse monoclonal detection antibody (MABX5523) were obtained from Sigma-Aldrich. Alexa Fluor® 430 NHS ester, used for antibody labeling, was obtained from ThermoFisher Scientific. An ATTO 430-labeled PSA-specific DNA aptamer (sequence: 5′-TTTTTAAT-TAAAGCTCGCCATCAAATAGCTT-3′) was acquired from Eurogentec.

The IL tetrabutylammonium chloride ($[N_{4444}]Cl$, ≥97 wt% purity) was combined with a phosphate buffer (pH ≈ 7) containing a 1.33:1 (w/w) mixture of potassium phosphate dibasic (K_2HPO_4, >98 wt% purity) and monobasic (KH_2PO_4, 99.5 wt% purity) at ca. 40 wt%, all from Sigma-Aldrich, to prepare the IL-ABS. Human serum was acquired from Sigma-Aldrich (H4522) and stored at −20 °C until use. PBS (pH ≈ 7.4) was prepared using pellets from Sigma-Aldrich according to manufacturer's instructions.

2.2. Fabrication of microfluidic devices

Polydimethylsiloxane (PDMS) microfluidic devices were fabricated using a standard soft lithography technique. The PDMS was obtained from Dow Corning (Midland, MI, USA) as part of the Sylgard® 184 elastomer kit. The fabrication process followed the methodology

described by Soares et al. [25], comprising three main steps: fabrication of aluminum hard masks, production of an SU-8 mold, and casting of the PDMS structures via soft lithography. The hard masks were fabricated by patterning aluminum-coated glass substrates using optical lithography followed by wet chemical etching. As the microfluidic device was designed to include an enclosed chamber for microbead trapping, two separate hard masks were required to create a dual-height microfluidic column. For mold fabrication, a clean silicon wafer (University Wafer, South Boston, MA, USA) was spin-coated with a 20 μm thick SU-8 2015 photoresist layer (Microchem Corp., Newton, MA, USA), soft-baked at 95 °C for 4 min and aligned with the first aluminum mask. Following UV exposure, a second bake was performed at 95 °C for 5 min. The patterned layer was then developed in propylene glycol monomethyl ether acetate (PGMEA), rinsed with isopropanol (IPA), and dried with nitrogen. A second SU-8 layer (SU-8 50, Microchem Corp.) was deposited on top of the first to achieve a final thickness of 100 μm, soft-baked at 65 °C for 10 min and 95 °C for 30 min. The second aluminum mask was aligned with the underlying pattern, exposed to UV light, and post-exposure baked at 65 °C for 1 min and 95 °C for 10 min. After development in PGMEA and rinsing with IPA, a final hard bake at 150 °C for 15 min was performed resulting in the final SU-8 mold. PDMS was prepared by mixing the base and curing agent in a 10:1 ratio, degassed under vacuum, poured over the SU-8 mold, and cured at 70 °C for 1.5 h. After curing, the PDMS layer was carefully peeled off the mold, and access ports for inlets and outlets were punched. The structure was then irreversibly bonded to a 500 μm-thick PDMS membrane using an oxygen plasma cleaner (Harrick Plasma, Ithaca, NY, USA).

A schematic representation of the device for PSA detection is shown in Fig. 1. The final device consisted of an array of 20 dual-height microchannels (Fig. 1A). Each device included a 20 μm-deep section and a 100 μm-deep region, allowing for the effective packing of protein G microbeads (~90 μm diameter, Fig. 1B). The shallower section served as a physical barrier, preventing beads from flowing downstream and forming a packed bed at the interface. Beads were introduced through a larger inlet chamber, which was sealed with a plug after packing. The immunoassay was subsequently carried out in the smaller chamber, with the remaining ports serving as fluid inlet and outlet. This design enabled precise control of flow and efficient interaction between the packed beads and assay reagents.

2.3. Fluid manipulation and microscopic images acquisition

Fluid flow within the microchannels was established using a NE-1002X syringe pump (New Era Pump Systems, Inc., NY, USA) equipped with 1 mL syringes (U-100, CODAN, Germany). The syringes were connected to a 20-gauge luer stub adapter and BTPE-60 polyethylene tubing (Instech Laboratories, PA, USA). An open metal adapter (Instech Laboratories, Inc., Montgomery, PA, USA) enabled the connection between the tubing and the microchannel outlet. Negative pressure generated by the syringe pump allowed for controlled fluid flow from the inlet to the outlet.

Fluorescence imaging was captured using a Leica DMLM microscope equipped with a DFC300FX digital camera. Alexa Fluor® 430 and ATTO 430-labeled molecules were visualized using a blue light excitation filter (450–490 nm). Images were acquired with a 1×-second exposure time, 10× magnification, and 1× gain. Fluorescence intensity was quantified using ImageJ software (National Institutes of Health, USA) by calculating the difference between the mean signal inside the channel and the background signal outside the channel. The values reported correspond to the average of two independent experiments.

2.4. Detection of PSA using microfluidic immunoassays

A microfluidic sandwich immunoassay was developed for the quantitative detection of PSA using either antibody-antibody or antibody-aptamer formats to mediate specific capture along with molecular recognition and detection. The antibodies were prepared in PBS, whereas the aptamer was prepared in Tris-buffered saline (TBS) composed of 10 mM Tris(hydroxymethyl)aminomethane hydrochloride, 150 mM sodium chloride, 5 mM potassium chloride, and 5 mM magnesium chloride. The assay began by packing Protein G-functionalized microbeads into the microchannel at 8 μL min^{-1} for 3 min, ensuring uniform bead distribution. Residual unbound material was removed with a PBS wash at the same flow rate for an additional 3 min. To functionalize the beads, a solution of capture anti-PSA antibody (100 μL min^{-1}) was pumped at a controlled flow rate of 0.5 μL min^{-1} for 10 min. To block non-specific interaction sites, a 1 mg min^{-1} human IgG solution was subsequently introduced for the antibody-antibody immunoassay, and a 0.5 % Tween-20 solution was used for the aptamer-based immunoassay, both at flow rate of 0.5 μL min^{-1} for 10 min. PSA standards, prepared in concentrations from 5 to 25 ng mL^{-1}, covering the clinically relevant concentration range [4], were pumped at 0.5 μL min^{-1} for 10 min to allow specific antigen binding. For each experimental condition, negative controls (0 ng min^{-1} of PSA) were analyzed in parallel to define the assay's background fluorescence. Detection was performed by introducing either a fluorescently labeled anti-PSA antibody (100 μL min^{-1}) or a fluorescently labeled PSA-specific aptamer (5 μM or 10 μM), both infused at 0.5 μL min^{-1} for 10 min. After each assay step, PBS was pumped through the microchannel at 5 μL min^{-1} for 1 min to minimize non-specific binding and maintain assay consistency. A schematic

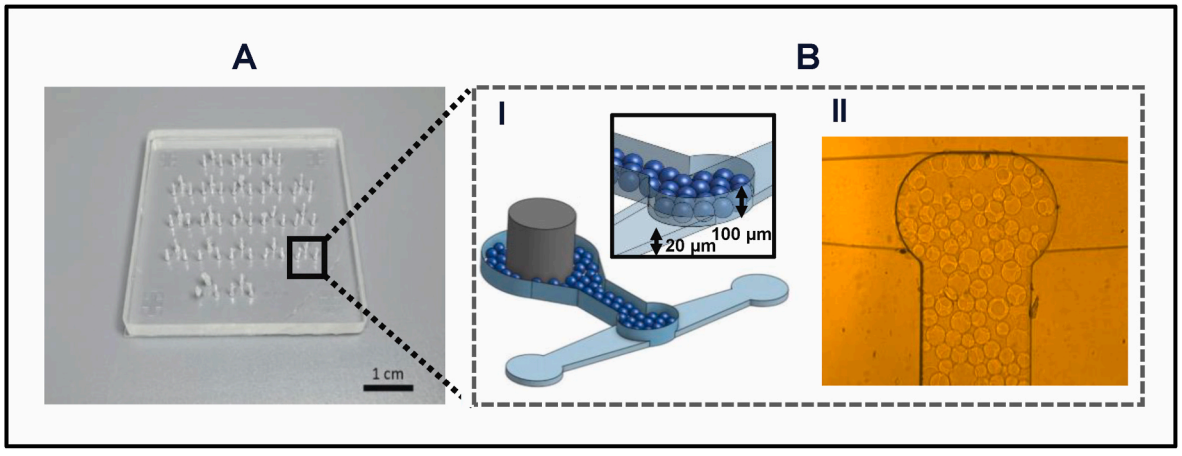

Fig. 1. Microfluidic device designed for PSA detection. (A) The final device consists of an array of 20 microchannels with dual-height architecture. (B) Each microchannel includes a 20 μm-height section and a 100 μm-height chamber designed to trap protein G-coated microbeads (I), as shown in the representative bright-field image acquired using a Leica microscope that depicts the microbeads retained (II).

representation of the sequential assay steps described is shown in Fig. 2.

Fluorescence intensity measurements were used to establish calibration curves for PSA detection in different sample environments, including PBS, untreated human serum, IL-ABS phases and IL-ABS pretreated serum.

The IL-ABS investigated comprised a mixture containing 30 wt% $[N_{4444}]Cl$, 12 wt% K_2HPO_4/KH_2PO_4 (salts only; buffer water included in the aqueous component), 10 wt% human serum spiked with PSA and 48 wt% water, and was applied to pretreat human serum prior to PSA analysis [23,24]. Briefly, the selection of this composition was guided by the ternary phase diagram previously reported for the corresponding IL-ABS, ensuring the formation of two immiscible aqueous phases (Fig. 3) [26]. Fig. 3A depicts the phase diagram, highlighting the selected biphasic system, with the IL structure shown in Fig. 3B to assist formulation design [26,27].

Previous work from our group has demonstrated that distinct ABS formulations exhibit different performances, both in terms of compatibility with microfluidic detection immunoassays and efficiency as sample pretreatment strategies [23,24]. These studies explored a variety of ILs, including imidazolium-, quaternary ammonium-, and phosphonium-based ILs, combined with phosphate- or citrate-based buffers. Within these broader screenings, the selected system consistently showed the most favourable profile, justifying its choice for the present application.

The IL-ABS was prepared to a final mass of 1 g by weighing and mixing the appropriate amounts of each constituent, followed by centrifugation for 10 min at 3500 rpm. Upon addition of human serum, the system selectively depletes the major serum proteins IgG and HSA through interfacial precipitation, resulting in the formation of a third, solid phase. Simultaneously, PSA is quantitatively extracted into the $[N_{4444}]Cl$-rich aqueous phase. Following phase separation, the IL-rich phase was collected and subsequently introduced into the microfluidic PSA detection device.

The assay sensitivity and limits of detection (LoD) were established by identifying the lowest PSA concentration yielding a fluorescence signal exceeding three times the standard deviation of the baseline from the negative control. This systematic approach allowed comparative analysis of PSA detection efficiency across various matrices, contributing to a deeper understanding of matrix effects on immunoassay performance and enabling the comparison between the aptamer and antibody as detection molecules.

3. Results and discussion

In this work, a microfluidic sandwich immunoassay was established to enable the quantitative detection of PSA using two distinct detection strategies: a conventional antibody-antibody format and an alternative antibody-aptamer format, in which the detection antibody is replaced by a PSA-specific aptamer. This established aptamer is used in a novel microfluidic format in combination with off-chip IL-ABS pretreatment [28].

This dual approach enabled a direct comparison of antibody-based and aptamer-based detection within the same optimized microfluidic platform. In addition, their integration with an off-chip IL-ABS pretreatment provided the opportunity to evaluate how selective serum cleanup and PSA extraction affect downstream detection. This pretreatment step streamlined serum handling by selectively precipitating high-abundance proteins at the system's interphase and transferring 100 % PSA into the top (IL-rich) phase [23], highlighting the added value of coupling IL-ABS with microfluidics for enhanced bioanalytical performance. Moreover, the IL used to form the ABS, $[N_{4444}]Cl$, in which PSA is extracted, is water-soluble, cost-effective and safe, supporting an aqueous, low-reagent, organic-solvent-free workflow consistent with green sample preparation principles [23,29]. Belonging to the quaternary ammonium family, its four butyl chains attached to the central nitrogen atom (Fig. 3B), together with the K_2HPO_4/KH_2PO_4 buffer, contribute to the precipitation of high-abundance serum proteins. Furthermore, the ammonium cation-chloride anion pair establishes a balance of properties that preserves PSA stability and solubility in the IL-rich phase [23]. Fig. 4 presents the conceptual workflow developed for PSA detection.

3.1. Conventional antibody-based immunoassay

Prior to performance testing, two platform modifications were implemented to improve assay robustness in the microfluidic format. The detection chamber was reconfigured from the previously used extended geometry (length = 3 mm; width = 700 μm) to a more compact

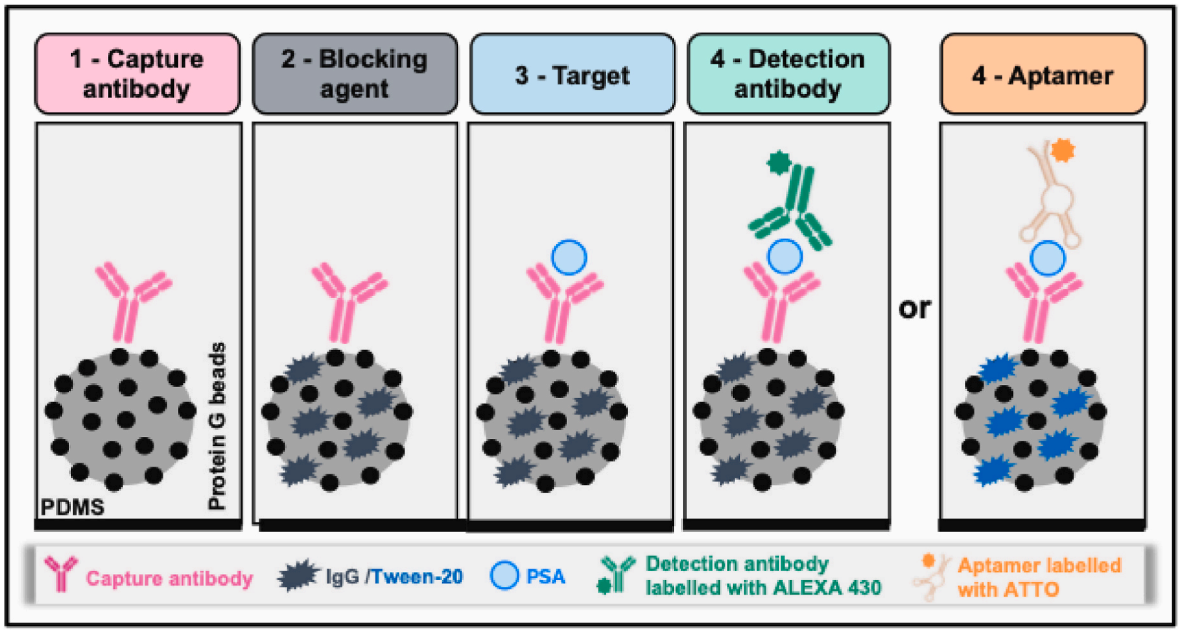

Fig. 2. Sequential steps of the microfluidic sandwich immunoassay for PSA detection using either a fluorescent anti-PSA detection antibody or a PSA-specific aptamer.

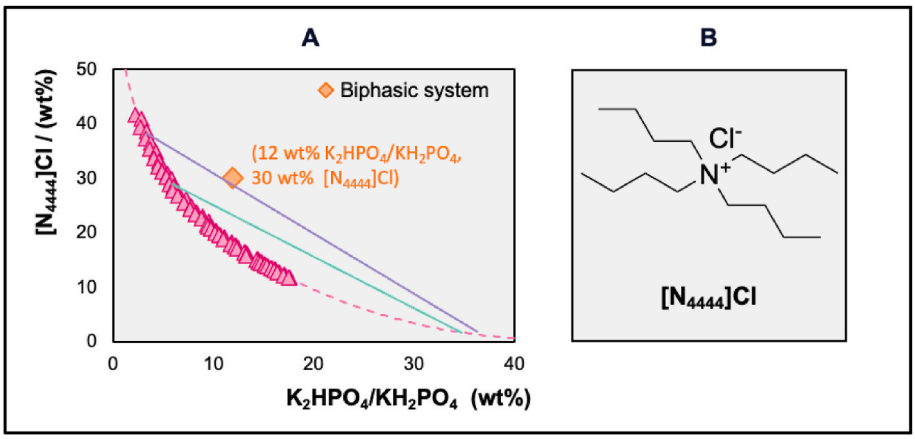

Fig. 3. Technical guide for IL-ABS preparation and serum pretreatment. (A) Ternary phase diagram of the $[N_{4444}]Cl$ plus K_2HPO_4/KH_2PO_4 ABS (pH ≈ 7). The experimental binodal data, shown as pink triangles and fitted using the Merchuk equation [27] (dashed pink line), separate biphasic from monophasic mixtures, located above and below the curve, respectively. Two tie-lines, determined via the gravimetric method proposed by the same author [27], are shown in green and purple, indicating the equilibrium compositions of the coexisting aqueous phases for a given mixture located along each line. The adopted biphasic mixture composition is marked by a orange diamond. Data were taken from the literature [26], where further experimental details and calculations can be found. (B) Chemical structure of $[N_{4444}]Cl$. (For interpretation of the references to colour in this figure legend, the reader is referred to the Web version of this article.)

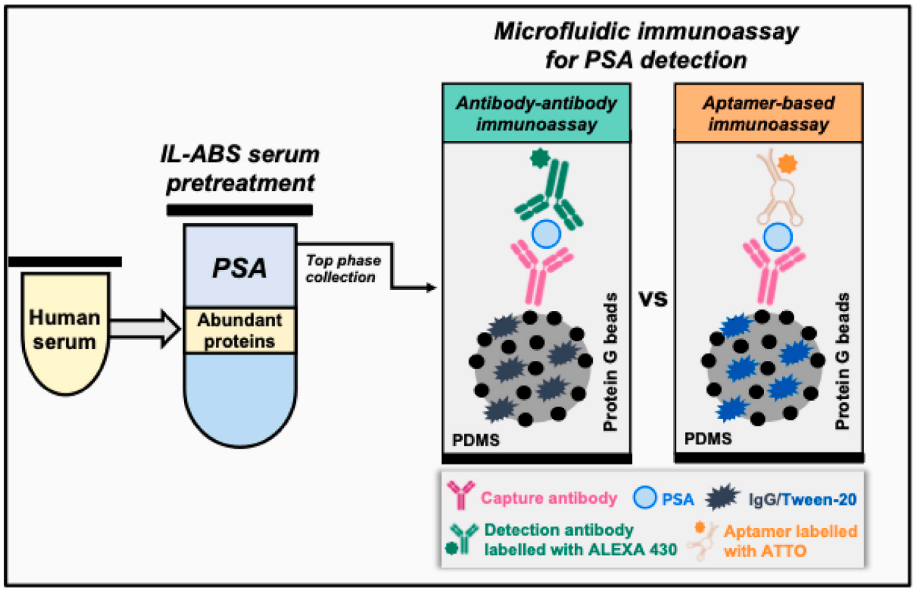

Fig. 4. Workflow for PSA detection combining IL-ABS human serum pretreatment with microfluidic immunoassays, comparing conventional antibody-antibody sandwich detection with the alternative antibody-aptamer strategy.

detection zone (length = 600 μm; width = 400 μm) to optimize diffusion dynamics and spatial signal uniformity [24]. In addition, bovine serum albumin (BSA) was replaced by IgG as the blocking agent, since BSA induced clogging in the reduced chamber geometry [24].

The performance of the antibody-antibody sandwich immunoassay for PSA detection was firstly evaluated both in PBS and in human serum without any sample pretreatment to establish baseline performance (Fig. 5). Detailed data is provided in Table S1 in the Supplementary Material. As shown in Fig. 5A, in PBS, the presence of 25 ng mL^{-1} of PSA resulted in a clear fluorescence signal increase, with an approximately 2.18-fold higher intensity compared to the negative control (0 ng mL^{-1}). In contrast, when the same assay was applied to human serum, there was no increase in signal upon PSA addition, preventing the construction of a reliable sensitivity curve. The higher signal in the negative control suggests that matrix components may enhance nonspecific background or hinder specific antibody binding, ultimately compromising assay sensitivity. These findings highlight the well-established performance of the antibody-antibody sandwich immunoassay in PBS and point to the challenges of translating the assay into human serum, where matrix effects can significantly impact detection efficiency.

To mitigate the pronounced matrix interference observed in untreated human serum, IL-ABS was implemented as a sample pretreatment strategy. The efficiency of IL-ABS pretreatment was evaluated by comparing PSA sensitivity curves under three conditions: (I) PSA diluted in PBS, representing the standard assay medium; (II) PSA spiked directly into the top (IL-rich) phase of an IL-ABS without biological contaminants, simulating ideal assay compatibility with the IL-ABS matrix; and (III) PSA extracted into the top (IL-rich) phase of an IL-ABS following pretreatment of PSA-spiked human serum, representing the practical application scenario. The fluorescence signals and resulting analytical parameters obtained in each condition are presented in Fig. 5B.

IL-ABS pretreatment substantially reduced matrix interference and enabled PSA quantification in serum preserving its availability. PSA diluted in PBS yielded the highest LoD at 17.72 ng mL^{-1}, reflecting poor

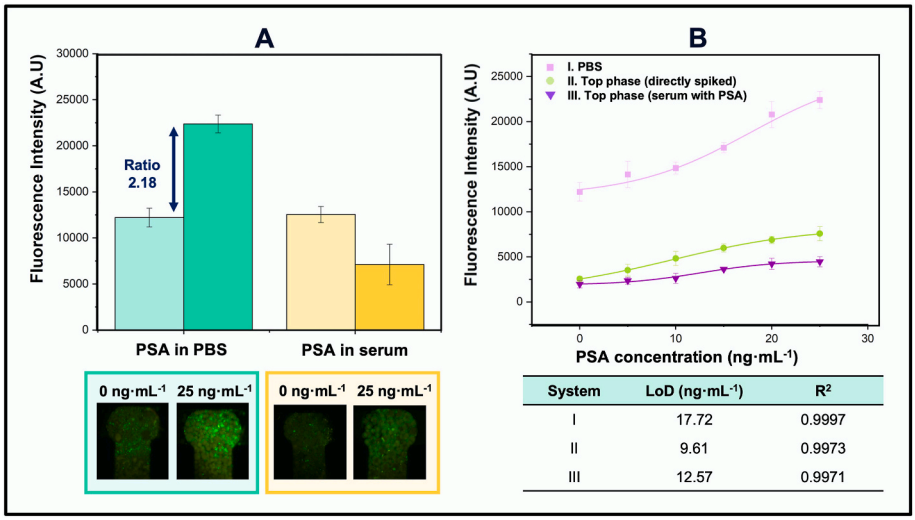

System	LoD (ng·mL^{-1})	R^2
I	17.72	0.9997
II	9.61	0.9973
III	12.57	0.9971

Fig. 5. Antibody-antibody sandwich immunoassay for PSA detection. (A) Fluorescence signal for 0 ng mL^{-1} of PSA in PBS and human serum (light green and yellow bars, respectively) and for 25 ng mL^{-1} of PSA (dark bars). Representative fluorescence images of the microfluidic detection zones are shown below each bar. (B) Calibration curves for PSA detection in PBS (I), IL-ABS top (IL-rich) phase spiked with PSA (II), and IL-ABS top (IL-rich) phase after serum pretreatment (III). The corresponding LoD and R^2 are shown in the table. (For interpretation of the references to colour in this figure legend, the reader is referred to the Web version of this article.)

sensitivity due to matrix-independent baseline interference. This high baseline in PBS likely arises from nonspecific adsorption of detection antibodies to Protein G beads or microchannel surfaces [24]. In contrast, PSA spiked directly into the clean top (IL-rich) phase achieved the lowest LoD of 9.61 ng mL^{-1}, confirming compatibility with the immunoassay. While PSA was essentially undetectable in untreated human serum, IL-ABS pretreatment allowed its extraction and quantification with a significantly improved LoD of 12.57 ng mL^{-1}. These results corroborate the beneficial role of IL-ABS and align with earlier reports using alternative microfluidic architectures [24].

Although IL-ABS successfully restores assay functionality in serum, further optimization is required to meet clinical thresholds. To this end, two complementary directions are here explored: besides device refinement, replacing the detection antibodies with aptamers as recognition molecules emerges as a promising strategy for performance enhancement. Owing to their distinctive physicochemical properties, aptamers are expected to improve binding efficiency and analytical sensitivity [30]. Overall, the optimized microfluidic architecture establishes a solid basis for subsequent integration of aptamer-based assays, further advancing the platform toward clinically viable PSA detection.

3.2. Aptamer-based immunoassay

The microfluidic detection of PSA using the aptamer-based immunoassay began with the preparation of the aptamer, a step that proved critical for ensuring its binding capacity. To investigate the impact of folding conditions, two aptamer preparation protocols were compared, as depicted in Fig. 6.

In Approach 1, the aptamer solution was heated at 95 °C for 10 min and then cooled slowly at room temperature for 10 min before incubation with PSA. This procedure resulted in no detectable fluorescence

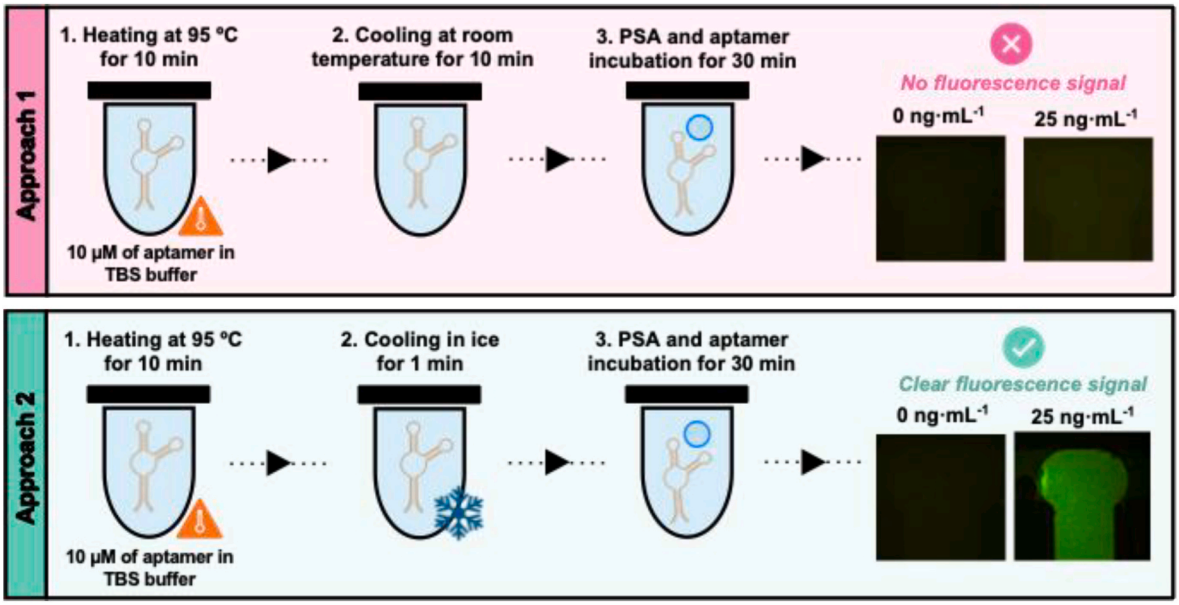

Fig. 6. Effect of aptamer preparation conditions on PSA recognition in the microfluidic assay.

signal, indicating that the aptamer was unable to recognize PSA under these conditions. In contrast, in Approach 2, the aptamer underwent the same heat treatment but was rapidly cooled on ice for 1 min prior to PSA incubation. This snap-cooling approach led to a clear fluorescence signal, confirming successful aptamer-PSA interaction. These results support the critical role of folding conditions in preserving the aptamer's functional structure [31]. While slow cooling likely promoted misfolding or formation of inactive conformers, rapid cooling favored the correct folding pathway necessary for target binding [31]. Because the stability of the aptamer's folded structure over time was not evaluated, the conformational preparation step was carried out immediately before each experiment to ensure consistent folding and reliable performance.

Following the optimization of the aptamer folding conditions, the influence of aptamer concentration and pre-incubation with PSA on assay performance was evaluated (Fig. 7), with detailed data provided in Table S2 in the Supplementary Material. Two aptamer concentrations (5 μM and 10 μM) were compared, and the effect of including a pre-incubation step with PSA was assessed to determine its impact on signal generation.

Since the aptamer acts as the detection molecule and must first bind PSA in solution, it was incubated with PSA alone rather than together with the capture antibody. This approach ensures that the capture antibody is immobilized before interacting with the target and provides a controlled environment that preserves proper aptamer folding and binding, both of which are essential for optimal assay performance. When the aptamer was pre-incubated with PSA for 30 min before detection, both concentrations yielded a marked fluorescence increase in the presence of PSA. The 10 μM aptamer with pre-incubation condition resulted in the highest fluorescence intensity, corresponding to a 19.24-fold increase relative to the negative control (0 ng mL^{-1} of PSA). The 5 μM aptamer with pre-incubation also produced a strong signal, with a 7.89-fold increase, but significantly lower compared to the 10 μM condition. In contrast, when the aptamer was not pre-incubated with PSA, the fluorescence signals were substantially reduced. The 10 μM aptamer without pre-incubation yielded only a 2.25-fold signal increase, while the 5 μM condition showed a 3.16-fold increase. These results clearly indicate that pre-incubation of the aptamer with PSA is essential to maximize binding efficiency and signal generation in the microfluidic assay. Altogether, these results confirm that both higher aptamer concentration and pre-incubation with the target are key parameters for optimal assay sensitivity. Pre-incubation likely promotes the formation of stable aptamer-PSA complexes prior to immobilization on the capture antibody, enhancing the overall detection performance.

After defining the optimal conditions using 10 μM aptamer with a 30-min pre-incubation with PSA, the performance of the aptamer-based microfluidic assay was assessed in human serum, as shown in Fig. 8 and detailed in Table S3 in the Supplementary Material.

The replacement of the detection antibody with an aptamer in the immunoassay format resulted in a strong signal enhancement in buffer conditions, demonstrating the aptamer's ability to bind PSA with high specificity and efficiency. In PBS, the assay achieved a signal-to-blank ratio close to 20 (Fig. 8A), indicating a robust fluorescence response and low background interference. This strong performance highlights the potential of aptamers as effective recognition elements, particularly given their advantages in terms of stability, cost, and ease of synthesis. However, the assay's performance was substantially hindered when applied directly to human serum. In this complex matrix, the signal-to-blank ratio dropped significantly to approximately 2.9, suggesting a pronounced matrix effect. This reduction is likely caused by competitive binding by high-abundance serum proteins or quenching of the fluorescence signal due to the presence of interfering biomolecules [32,33]. These effects are commonly observed in complex biological samples, representing a key challenge in translating aptamer-based assays to clinical contexts.

As shown in the sensitivity curves in Fig. 8B, the assay maintained high sensitivity in PBS, while direct detection in untreated serum resulted in lower signal intensity and higher variability. The most significant enhancement was observed when human serum was first subjected to the same IL-ABS previously applied in the antibody-antibody immunoassay, and the resulting top (IL-rich) phase, considerably depleted of high-abundance serum proteins, was then used for PSA detection. In this condition, the aptamer-based assay achieved a marked improvement in analytical performance, with a lower LoD (7.49 ng mL^{-1}). These findings suggest that the IL-ABS pretreatment effectively overcomes aptamer target binding limitations, improving assay robustness and performance in complex biological matrices. In contrast to conventional pretreatment strategies such as SPE, which typically involve multiple binding, washing, and elution steps [17], IL-ABS also enables protein depletion and target isolation in a single, rapid step with minimal sample handling. Moreover, SPE often relies on specific sorbent chemistries that may lead to nonspecific losses of biomarkers or partial denaturation [34], compromising aptamer recognition. Using $[N_{4444}]Cl$, IL-ABS functions under gentle aqueous conditions without requiring solid supports, avoing these issues and preserving biomolecular structure [23].

In comparison with the antibody-antibody immunoassay, the aptamer-based format demonstrated superior sensitivity and lower LoD (7.49 ng mL^{-1} vs 12.57 ng mL^{-1}) under identical pretreatment and microfluidic detection conditions. This result is particularly relevant, as the LoD falls within the clinically relevant range for PSA detection,

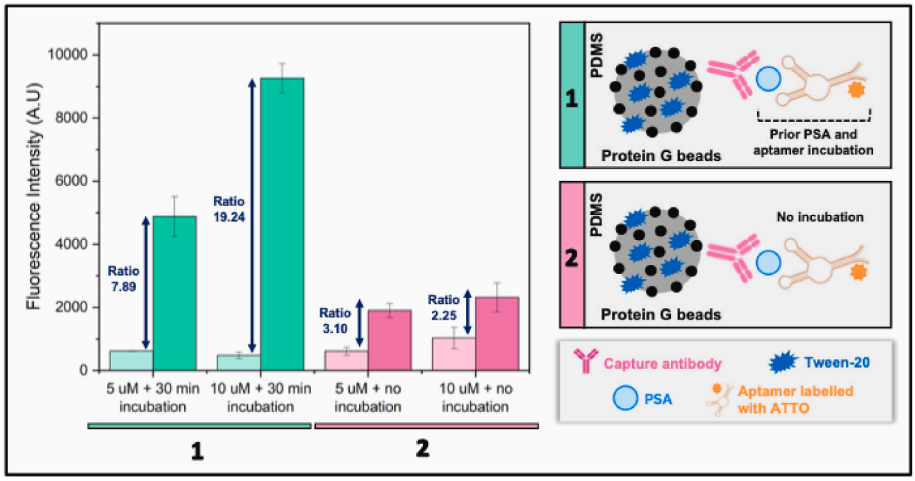

Fig. 7. Effect of aptamer concentration and pre-incubation with PSA on fluorescence signal in the microfluidic aptamer-based immunoassay.

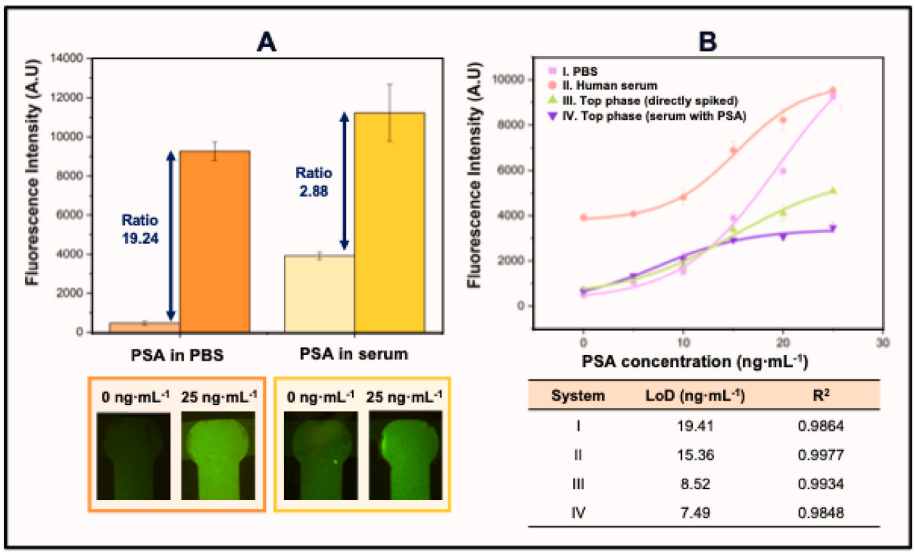

System	LoD (ng·mL^{-1})	R^2
I	19.41	0.9864
II	15.36	0.9977
III	8.52	0.9934
IV	7.49	0.9848

Fig. 8. Aptamer-based immunoassay for PSA detection. (A) Comparison of fluorescence signals obtained in PBS and human serum. Representative fluorescence images of the microfluidic detection zones are shown below each bar. Negative controls are represented by the lighter orange and yellow bars for PBS and serum, respectively, while the corresponding positive controls containing 25 ng mL^{-1} of PSA are shown in darker shades of orange and yellow. (B) Sensitivity curves for PSA detection in PBS (I), human serum (II), top (IL-rich) phase of an IL-ABS spiked with PSA (III), and top (IL-rich) phase of an IL-ABS after serum pretreatment (IV). The LoD and R^2 for each condition are summarized in the table. (For interpretation of the references to colour in this figure legend, the reader is referred to the Web version of this article.)

which typically spans from 4 to 11 ng mL^{-1} [4]. These improvements can be attributed to several inherent advantages of aptamers. For example, their smaller molecular size allows for closer proximity between the recognition (aptamer) and fluorescent reporter (ATTO 430) elements, enhancing fluorescence signal transduction in complex serum samples. Aptamers also exhibit greater stability over a broader range of temperatures and pH, which is particularly advantageous for point-of-care settings, where the window of controllable experimental conditions is narrower than in centralized laboratories. Furthermore, aptamers are less prone to batch-to-batch variation and can be chemically modified to improve assay reproducibility and enable customization, supporting reliable diagnostics in decentralized clinical contexts. Additionally, their synthetic nature allows for scalable and ethically sound production, facilitating broader translation of the platform to clinical and point-of-care applications.

Finally, current clinical analyses for PSA quantification rely on immunoassays performed on automated platforms, which offer high sensitivity and accuracy but require specialized equipment, trained personnel, and long turnaround times [4]. These limitations reduce their suitability for decentralized care and delay immediate clinical decisions [35]. In contrast, rapid tests provide faster and more accessible PSA evaluation, often at the cost of sensitivity and with susceptibility to matrix effects [4]. Incorporating this IL-ABS pretreatment improves signal-to-noise ratios and enhances PSA detection via microfluidic platforms, with the potential for portability and user-friendly operation. The combination of speed, simplicity, and analytical performance demonstrates how the proposed approach could outperform current methods, enabling more sensitive and reliable PSA analysis in clinical and point-of-care settings.

4. Conclusions

This work shows the successful combination of IL-ABS serum pretreatment with microfluidic technology for PSA detection, highlighting the expanded potential achieved with aptamer-based detection beyond conventional antibody-based strategies. By directly comparing traditional antibody-antibody and alternative antibody-aptamer sandwich immunoassays, it was confirmed that while both formats perform well in PBS, the aptamer-based approach consistently exhibited superior sensitivity and lower LoD, particularly under optimized folding conditions and pre-incubation with PSA. Both formats, however, suffered from signal attenuation in untreated human serum due to matrix interference. The implementation of IL-ABS as a pretreatment step effectively mitigated these effects by depleting high-abundance serum proteins and minimizing nonspecific interactions. By synergistically integrating off-chip IL-ABS pretreatment with microfluidics, PSA was detected down to 7.49 ng mL^{-1}, well within the clinically relevant range. The aptamer-based format delivered the best bioanalytical performance of this combined platform, validating a transformative potential that surpasses conventional antibody-based strategies.

Compared to earlier IL-ABS microfluidic platforms, the newly developed detection device features a more compact chamber, resulting in a more uniform fluorescence distribution and reduced spatial signal variability. Moreover, the use of aptamers provides enhanced stability, ease of modification, reduced production variability, and ethical manufacturing benefits over traditional antibodies, supporting their strong potential for clinical and point-of-care applications.

From the findings reported herein, the combination of aptamer recognition with IL-ABS sample pretreatment and microfluidic detection offers a robust framework for biomarker analysis in complex samples. Future improvements in assay design, aptamer engineering, and integration with portable readout systems could further enhance sensitivity and usability. Such refinements could accelerate the translation of this integrated platform into clinically and point-of-care viable PSA testing, while extending its applicability to a broader spectrum of protein biomarkers.

CRediT authorship contribution statement

Maria S.M. Mendes: Writing – original draft, Visualization, Validation, Methodology, Investigation, Formal analysis, Data curation. **Virginia Chu:** Writing – review & editing. **Mara G. Freire:** Writing – review & editing, Supervision, Funding acquisition, Conceptualization. **Francisca A. e Silva:** Writing – review & editing, Supervision, Project administration, Funding acquisition, Conceptualization. **João P. Conde:** Writing – review & editing, Supervision, Funding acquisition,

Conceptualization.

Declaration of competing interest

The authors declare that they have no known competing financial interests or personal relationships that could have appeared to influence the work reported in this paper.

Acknowledgements

The authors acknowledge Inês Agostinho for her help with the design and microfabrication of the microfluidic structures.

This work was developed within the scope of the project CICECO – Aveiro Institute of Materials, UID/50011/2025 (DOI 10.54499/UID/50011/2025) & LA/P/0006/2020 (DOI 10.54499/LA/P/0006/2020), financed by national funds through the FCT/MCTES (PIDDAC). INESC MN acknowledges plurianual financing from FCT through UID/PRR/5367/2025 and UID/5367/2025. This work was developed within the project ILSurvive, PTDC/EMD-TLM/3253/2020 (DOI 10.54499/PTDC/EMD-TLM/3253/2020), funded by national funds (OE), through FCT/MCTES. M.S.M.M. acknowledges FCT for the doctoral grant 2022.11229.BD (DOI 10.54499/2022.11229.BD). F.A.eS. acknowledges FCT for the researcher contract CEECIND/03076/2018/CP1559/CT0024 (DOI 10.54499/CEECIND/03076/2018/CP1559/CT0024) under the Scientific Employment Stimulus – Individual Call 2018.

Appendix A. Supplementary data

Supplementary data to this article can be found online at https://doi.org/10.1016/j.aca.2025.345001.

Data availability

Data will be made available on request.

References

[1] F. Bray, M. Laversanne, H. Sung, J. Ferlay, R.L. Siegel, I. Soerjomataram, A. Jemal, Global cancer statistics 2022: GLOBOCAN estimates of incidence and mortality worldwide for 36 cancers in 185 countries, CA Cancer J. Clin. 74 (2024) 229–263, https://doi.org/10.3322/caac.21834.

[2] M.W. Farha, S.S. Salami, Biomarkers for prostate cancer detection and risk stratification, Ther Adv Urol 14 (2022), https://doi.org/10.1177/17562872221103988.

[3] J.F. Rusling, C.V. Kumar, J.S. Gutkind, V. Patel, Measurement of biomarker proteins for point-of-care early detection and monitoring of cancer, Analyst 135 (2010) 2496, https://doi.org/10.1039/c0an00204f.

[4] S. Garg, A. Sachdeva, M. Peeters, J. McClements, Point-of-Care prostate specific antigen testing: examining translational progress toward clinical implementation, ACS Sens. 8 (2023) 3643–3658, https://doi.org/10.1021/acssensors.3c01402.

[5] Z. Liu, X. Han, L. Qin, Recent progress of microfluidics in translational applications, Adv. Healthcare Mater. 5 (2016) 871–888, https://doi.org/10.1002/adhm.201600009.

[6] T. Matsunaga, Y. Maeda, T. Yoshino, H. Takeyama, M. Takahashi, H. Ginya, J. Aasahina, H. Tajima, Fully automated immunoassay for detection of prostate-specific antigen using nano-magnetic beads and micro-polystyrene bead composites, 'beads on beads, Anal. Chim. Acta 597 (2007) 331–339, https://doi.org/10.1016/j.aca.2007.05.065.

[7] D.E. Bernstein, J. Piedad, L. Hemsworth, A. West, I.D. Johnston, N. Dimov, J. M. Inal, N. Vasdev, Prostate cancer and microfluids, Urol. Oncol.: Seminars and Original Investigations 39 (2021) 455–470, https://doi.org/10.1016/j.urolonc.2021.03.010.

[8] N.V. Panini, G.A. Messina, E. Salinas, H. Fernández, J. Raba, Integrated microfluidic systems with an immunosensor modified with carbon nanotubes for detection of prostate specific antigen (PSA) in human serum samples, Biosens. Bioelectron. 23 (2008) 1145–1151, https://doi.org/10.1016/j.bios.2007.11.003.

[9] N. Triroj, P. Jaroenapibal, H. Shi, J.I. Yeh, R. Beresford, Microfluidic chip-based nanoelectrode array as miniaturized biochemical sensing platform for prostate-specific antigen detection, Biosens. Bioelectron. 26 (2011) 2927–2933, https://doi.org/10.1016/j.bios.2010.11.039.

[10] S. Chen, Z. Wang, X. Cui, L. Jiang, Y. Zhi, X. Ding, Z. Nie, P. Zhou, D. Cui, Microfluidic device directly fabricated on screen-printed electrodes for ultrasensitive electrochemical sensing of PSA, Nanoscale Res. Lett. 14 (2019) 71, https://doi.org/10.1186/s11671-019-2857-6.

[11] T. Wang, C. Chen, L.M. Larcher, R.A. Barrero, R.N. Veedu, Three decades of nucleic acid aptamer technologies: lessons learned, progress and opportunities on aptamer development, Biotechnol. Adv. 37 (2019) 28–50, https://doi.org/10.1016/j.biotechadv.2018.11.001.

[12] Z. Chen, Y. Yang, X. Cui, L. Chai, H. Liu, Y. Pan, Y. Zhang, Y. Xie, T. Le, Process, advances, and perspectives of graphene oxide-SELEX for the development of aptamer molecular probes: a comprehensive review, Anal. Chim. Acta 1320 (2024) 343004, https://doi.org/10.1016/j.aca.2024.343004.

[13] F. Zhang, S. Li, K. Cao, P. Wang, Y. Su, X. Zhu, Y. Wan, A microfluidic love-wave biosensing device for PSA detection based on an aptamer beacon probe, Sensors 15 (2015) 13839–13850, https://doi.org/10.3390/s150613839.

[14] Q. Zhou, Y. Lin, K. Zhang, M. Li, D. Tang, Reduced graphene oxide/BiFeO3 nanohybrids-based signal-on photoelectrochemical sensing system for prostate-specific antigen detection coupling with magnetic microfluidic device, Biosens. Bioelectron. 101 (2018) 146–152, https://doi.org/10.1016/j.bios.2017.10.027.

[15] K. Björhall, T. Miliotis, P. Davidsson, Comparison of different depletion strategies for improved resolution in proteomic analysis of human serum samples, Proteomics 5 (2005) 307–317, https://doi.org/10.1002/pmic.200400900.

[16] H.J. Issaq, T.D. Veenstra, Sample depletion, fractionation, and enrichment for biomarker discovery, in: Proteomic and Metabolomic Approaches to Biomarker Discovery, Elsevier, 2020, pp. 95–102, https://doi.org/10.1016/B978-0-12-394446-7.00015-7.

[17] V. Polaskova, A. Kapur, A. Khan, M.P. Molloy, M.S. Baker, High-abundance protein depletion: comparison of methods for human plasma biomarker discovery, Electrophoresis 31 (2010) 471–482, https://doi.org/10.1002/elps.200900286.

[18] M.S.M. Mendes, M.E. Rosa, F. Ramalho, M.G. Freire, F.A. e Silva, Aqueous two-phase systems as multipurpose tools to improve biomarker analysis, Sep. Purif. Technol. 317 (2023) 123875, https://doi.org/10.1016/j.seppur.2023.123875.

[19] M. Garza-Madrid, M. Rito-Palomares, S.O. Serna-Saldívar, J. Benavides, Potential of aqueous two-phase systems constructed on flexible devices: human serum albumin as proof of concept, Process Biochem. 45 (2010) 1082–1087, https://doi.org/10.1016/j.procbio.2010.03.026.

[20] A. Mahn, M.E. Lienqueo, C. Quilodrán, A. Olivera-Nappa, Purification of transthyretin as nutritional biomarker of selenium status, J. Separ. Sci. 35 (2012) 3184–3189, https://doi.org/10.1002/jssc.201200646.

[21] T. Yao, J. Liu, M. Feng, C. Feng, Extraction of aloe polysaccharides by recoverable aqueous biphasic system composed of thermo-sensitive magnetic ionic liquid and pH-sensitive copolymer, J. Chromatogr. A 1759 (2025) 466249, https://doi.org/10.1016/j.chroma.2025.466249.

[22] T. Yao, C. Feng, Y. Hu, S. Yang, Isolation and purification of aloe anthraquinones through recoverable triple-responsive aqueous two-phase system, Sep. Purif. Technol. 374 (2025) 133786, https://doi.org/10.1016/j.seppur.2025.133786.

[23] M.E. Rosa, M.S.M. Mendes, E. Carmo, J.P. Conde, J.A.P. Coutinho, M.G. Freire, F. A. e Silva, Tailored pretreatment of serum samples and biomarker extraction afforded by ionic liquids as constituents of aqueous biphasic systems, Sep. Purif. Technol. 322 (2023) 124248, https://doi.org/10.1016/j.seppur.2023.124248.

[24] F.C. Flora, S.B. Relvas, F.A. e Silva, M.G. Freire, V. Chu, J.P. Conde, Combined use of ionic liquid-based aqueous biphasic systems and microfluidic devices for the detection of prostate-specific antigen, Biosensors (Basel) 13 (2023) 334, https://doi.org/10.3390/bios13030334.

[25] R.R.G. Soares, P. Novo, A.M. Azevedo, P. Fernandes, M.R. Aires-Barros, V. Chu, J. P. Conde, On-chip sample preparation and analyte quantification using a microfluidic aqueous two-phase extraction coupled with an immunoassay, Lab Chip 14 (2014) 4284–4294, https://doi.org/10.1039/c4lc00695j.

[26] D.C.V. Belchior, M.V. Quental, M.M. Pereira, C.M.N. Mendonça, I.F. Duarte, M. G. Freire, Performance of tetraalkylammonium-based ionic liquids as constituents of aqueous biphasic systems in the extraction of ovalbumin and lysozyme, Sep. Purif. Technol. 233 (2020) 116019, https://doi.org/10.1016/j.seppur.2019.116019.

[27] J.C. Merchuk, B.A. Andrews, J.A. Asenjo, Aqueous two-phase systems for protein separation studies on phase inversion, J. Chromatogr., B: Anal. Technol. Biomed. Life Sci. 711 (1998) 285–293, https://doi.org/10.1016/S0378-4347(97)00594-X.

[28] S. Zhao, J. Huang, D. Li, L. Yang, Aptamer-based chemiluminescent optical fiber immunosensor with enhanced signal amplification for ultrasensitive detection of tumor biomarkers, Biosens. Bioelectron. 214 (2022) 114505, https://doi.org/10.1016/j.bios.2022.114505.

[29] Á.I. López-Lorente, F. Pena-Pereira, S. Pedersen-Bjergaard, V.G. Zuin, S.A. Ozkan, E. Psillakis, The ten principles of green sample preparation, TrAC, Trends Anal. Chem. 148 (2022) 116530, https://doi.org/10.1016/j.trac.2022.116530.

[30] P. Jolly, P. Damborsky, N. Madaboosi, R.R.G. Soares, V. Chu, J.P. Conde, J. Katrlik, P. Estrela, DNA aptamer-based sandwich microfluidic assays for dual quantification and multi-glycan profiling of cancer biomarkers, Biosens. Bioelectron. 79 (2016) 313–319, https://doi.org/10.1016/j.bios.2015.12.058.

[31] M.D. Schump, D.I. Bernstein, F.J. Bravo, C.P. Neff, Selection, activity, and nuclease stabilization of cross-neutralizing DNA aptamers targeting HSV-1 and HSV-2, Virology 589 (2024) 109916, https://doi.org/10.1016/j.virol.2023.109916.

[32] B.-Y. Fang, J. An, B. Liu, Y.-D. Zhao, Hybridization induced fluorescence enhanced DNA-Ag nanocluster/aptamer probe for detection of prostate-specific antigen, Colloids Surf. B Biointerfaces 175 (2019) 358–364, https://doi.org/10.1016/j.colsurfb.2018.12.013.

[33] X. Wang, M. Zhao, D.D. Nolte, T.L. Ratliff, Prostate specific antigen detection in patient sera by fluorescence-free BioCD protein array, Biosens. Bioelectron. 26 (2011) 1871–1875, https://doi.org/10.1016/j.bios.2010.02.009.
[34] M.R. Bladergroen, Y.E.M. van der Burgt, Solid-phase extraction strategies to surmount body fluid sample complexity in high-throughput mass spectrometry-based proteomics, J Anal Methods Chem 2015 (2015) 1–8, https://doi.org/10.1155/2015/250131.
[35] B. Srinivasan, D.M. Nanus, D. Erickson, S. Mehta, Highly portable quantitative screening test for prostate-specific antigen at point of care, Curr Res Biotechnol 3 (2021) 288–299, https://doi.org/10.1016/j.crbiot.2021.11.003.